crystals

MDPI

Article

Elevated Temperature Mechanical Characteristics and Fracture Behavior of a Novel Beta Titanium Alloy

Seyed Vahid Sajadifar [1,2], Hans Jürgen Maier [3], Thomas Niendorf [2] and Guney Guven Yapici [1,*]

[1] Mechanical Engineering Department, Ozyegin University, 34794 Istanbul, Türkiye
[2] Institute of Materials Engineering, Metallic Materials, Universität Kassel, Mönchebergstraße 3, 34125 Kassel, Germany
[3] Institut für Werkstoffkunde (Materials Science), Leibniz Universität Hannover, 30823 Garbsen, Germany
* Correspondence: guven.yapici@ozyegin.edu.tr; Tel.: +90-216-5649115

Abstract: In the present work, the elevated-temperature deformation characteristics and microstructural evolution of a Ti-5V-5Mo-5Cr-4Al alloy in solution-treatment conditions were studied under a tensile load at temperatures in the range of 25 to 550 °C and strain rates between 0.001 and 0.1 s^{-1}. The results obtained indicated that, essentially, dynamic recovery (DRV) was the dominant softening mechanism in the case of the regimes considered. An analysis based on transmission electron microscopy (TEM) and the assessment of the mechanical behavior of the solution-heat-treated Ti-5V-5Mo-5Cr-4Al alloy revealed that dynamic precipitation (DPN) only took place at a strain rate of 0.001 s^{-1} and at temperatures of 450 °C and 500 °C. Void coalescence occurred upon an increase in the deformation temperature and a decrease in the strain rate due to a higher rate of diffusion and the provision of sufficient time for growth, respectively. The results obtained in the present study pave the way for the robust processing of this novel β titanium alloy. Depending on the deformation parameters, the deformation characteristics can be governed by either DRV (at moderate temperatures) or DPN (at moderate temperatures and at low rates of deformation).

Keywords: Ti-5V-5Mo-5Cr-4Al alloy; beta titanium; elevated temperature; mechanical behavior; dynamic recovery; dynamic precipitation; fracture morphology; forming

Citation: Sajadifar, S.V.; Maier, H.J.; Niendorf, T.; Yapici, G.G. Elevated Temperature Mechanical Characteristics and Fracture Behavior of a Novel Beta Titanium Alloy. *Crystals* **2023**, *13*, 269. https://doi.org/10.3390/cryst13020269

Academic Editors: Hongbin Bei and Malte Vollmer

Received: 14 January 2023
Revised: 28 January 2023
Accepted: 28 January 2023
Published: 3 February 2023

1. Introduction

Titanium (Ti) and its alloys are widely used in applications wherein a high specific strength in combination with favorable ductility is required. Commercial-purity titanium is not capable of being utilized in structures that require high strength. Therefore, β (beta) Ti alloys have been introduced as the best candidates for engineering applications demanding both high strength and formability [1,2]. The aerospace industry uses β Ti alloys for aircraft components owing to their extraordinary properties, reduced hazard of stress corrosion cracking, and relatively light weight [3,4]. Among the β titanium alloys, the quest for high strength while preserving ductility has led to the development of the Ti-5V-5Mo-5Cr-4Al alloy for aerospace applications.

Recently, the extremely high forces needing to be applied during the warm and hot rolling or forging of these materials, which were clearly detrimental to the efficiency of the processes, motivated researchers to initiate numerous investigations into the hot deformation characteristics of Ti alloys [2,5–17]. Studies on the hot deformation characteristics of the Ti-5Al-5Mo-5V-3Cr alloy in the temperature range of 750–900 °C revealed that the deformation parameters considerably influenced the microstructural changes and softening mechanisms, such as dynamic recovery (DRV) and dynamic recrystallization (DRX) [2]. With an increase in the deformation temperature, DRV and DRX took place, the former leading to an increase in the fraction of low-angle grain boundaries (LAGBs). The deformation behavior and microstructural evolution of biomedical Ti-13Nb-13Zr alloy at temperatures ranging from ambient to 800 °C and strain rates of 1000 s^{-1}, 2000 s^{-1}, and 3000 s^{-1} were

studied in another research work [14]. It was found that the flow stress levels dropped with an increasing deformation temperature and a decreasing rate of deformation [14]. Moreover, the warm deformation behavior of a metastable β Ti-Nb alloy was studied in [15]. The results showed that multiple deformation mechanisms, including mechanical twinning and dislocation slip, were active during warm deformation. In two separate studies, the tensile behaviors of the Ti-10V-2Fe-3Al and Ti-22Al-24Nb-0.5Mo β alloys were investigated up to a deformation temperature of 650 °C [16,17]. The dependency of fracture strain on the rate of deformation was reported for Ti-10V-2Fe-3Al [16]. In order to identify the failure mechanisms of materials in service, several studies focused on the fracture surface analysis of titanium alloys [16–20]. The fracture behavior of additively manufactured Ti-6Al-4V was compared to that of a wrought alloy, finally revealing anisotropic fractures for both cases [18]. Fracture surface analysis was also conducted for β Ti alloys after cyclic tests [19,21,22]. Fractography uncovered that microcrack initiation and strain concentration occurred at the α/β interfaces of Ti-5Al-5Mo-5V-3Cr-1Zr titanium alloy [19]. Fracture analysis of a Ti-5Al-5Mo-5V-1Cr-1Fe titanium alloy subjected to high-cycle fatigue (HCF) revealed that the area of the initiation region decreased in size in the sequence of coarse basketweave, fine basketweave, Widmanstätten, and bimodal microstructures [21]. Among the abovementioned works, only a few studies concentrated on the warm fracture behavior of Ti alloys [16,17,20]. Generally, void and dimple sizes grow when the deformation temperature is increased or the rate of deformation is reduced. The emerging risk of fracture has motivated researchers to predict the fracture behavior of β Ti alloys under different deformation conditions, and the Ti-10V-2Fe-3Al alloy was shown to have a lower risk of fracture at 700–750 °C and strain rates of 0.3162–3.1623 s^{-1} [23].

The assessment of the impact of the deformation parameters on the mechanical properties and microstructural evolution is an essential part of the in-depth analysis of β Ti alloys. To the best of the authors' knowledge, the warm mechanical behavior and subsequent fracture surface analysis of the Ti-5V-5Mo-5Cr-4Al alloy have not been studied thoroughly so far. The lack of discussion on this high-strength alloy was the main motivation for the present work. The warm deformation characteristics of this novel alloy were evaluated by conducting elevated-temperature tensile tests and fracture surface analysis. For this purpose, tensile tests were carried out at temperatures ranging from ambient to 550 °C and at various strain rates. The results obtained herein pave the way toward the robust fabrication of this novel beta titanium alloy in solution-heat-treated conditions.

2. Materials and Methods

The Ti-5V-5Mo-5Cr-4Al alloy was obtained in the form of extruded bars with the chemical composition listed in Table 1, as determined by optical emission spectroscopy (OES).

Table 1. Chemical composition of Ti-5V-5Mo-5Cr-4Al alloy studied in the present work.

Element	C	Fe	H	N	O	Al	V	Cr	Mo	Ti
Weight percent	0.002	0.06	0.002	0.01	0.08	4.0	5.0	5.4	5.2	Balance

Solution heat treatment was carried out at 900 °C ± 3 °C for 1 h, followed by water quenching. The test specimens were electro-discharge machined (EDM) with their loading axis parallel to the extrusion direction. Specimens featured a gage length of 15mm, as shown in Figure 1. All specimens were ground and polished to remove scratches and eliminate the influence of the EDM residual layer. The tensile tests were conducted under isothermal conditions at strain rates of 0.001, 0.01, and 0.1 s^{-1} and temperatures ranging from 25 to 550 °C. A servo-hydraulic Instron 8872 (Instron, High Wycombe, UK) mechanical test frame was employed for tensile experiments, where the movement of the crosshead was monitored continuously. Tensile experiments were conducted according to ASTM E8/E8M-21 [24]. All specimens were heated up to the deformation temperature and then

deformed in a single loading step. The specimen temperature was monitored during the tests using K-type thermocouples with a standard deviation of ±2.2 °C. Three tensile tests were conducted per condition to check the reproducibility of the data. The scatter of the data points was relatively low. Thus, only a single representative curve per condition is shown in the present work. Vickers microhardness tests were carried out on the specimens with 9.81 N force and a 10 s indentation duration at ambient temperature. Each microhardness value was obtained from an average of 5 indentations.

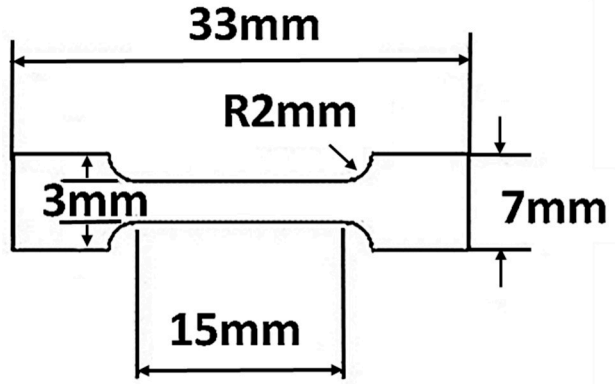

Figure 1. Specimen geometry used for tensile tests.

Optical microscopy (OM) was employed to monitor the changes in the microstructure. The specimens were prepared using standard polishing techniques and then etched with Kroll's reagent (3 mL HF + 6 mL HNO_3 in 100 mL distilled water). The linear intercept method was used to determine the grain size. Furthermore, a scanning electron microscope (SEM) operated at an accelerating voltage of 20 kV was used to analyze the microstructure as well as the fracture surfaces of specimens in different conditions. The microstructure of the Ti-5V-5Mo-5Cr-4Al alloy was further analyzed using transmission electron microscopy (TEM). For TEM analysis, specimens were first cut using a Struers Minitom low-speed diamond saw. Then, disks with diameters of 3 mm were punched. Disks were mechanically ground down to 100 µm. Electropolishing was conducted with an electrolyte comprising 20% perchloric acid + 80% ethanol solution at –30 °C and 15 V using a Struers-Tenupol-5 Double Jet Electropolisher (Struers, Copenhagen, Denmark). The electropolished specimens were additionally ion-milled, and the foils were studied with a JEOL JEM 2100 HR TEM operated at 200 kV.

3. Results and Discussion

3.1. Mechanical Behavior of Ti-5V-5Mo-5Cr-4Al Alloy

Figure 2 depicts the tensile stress–strain curves of the Ti-5V-5Mo-5Cr-4Al alloy at various temperatures ranging from ambient to 550 °C and at strain rates of 0.001 to 0.1 s^{-1}. The highest standard deviations of strain and stress were found to be 0.006 and 15.6 MPa, respectively. The dependence of the flow stress on the deformation temperature and the deformation rate was obvious. It can be deduced from Figure 2 that the flow stress level dropped with an increase in the deformation temperature at strain rates of 0.01 and 0.1 s^{-1}. It is well-known that DRV usually takes place at temperatures above 0.3 T_m, where T_m is the melting temperature on the Kelvin scale [7,25,26]. Therefore, the reduction in the flow stress level of the Ti-5V-5Mo-5Cr-4Al alloy upon an increase in the deformation temperature could be attributed to the occurrence of DRV. Unexpected behavior was observed at temperatures of 450 °C and 500 °C and a strain rate of 0.001 s^{-1}. At this rate of deformation (0.001 s^{-1}), the true ultimate tensile strength (UTS) significantly increased with the increase in temperature up to 550 °C. This behavior could be rationalized in terms of dynamic precipitation (DPN). It is well-documented that DPN occurs when a specimen is exposed to an intermediate temperature and superimposed external stress [27–29]. Since the 450 °C and 500 °C deformation temperatures were the aging temperatures of the

studied alloy, the abnormal deformation behavior observed for the specimens at 450 °C and 500 under a strain rate of 0.001 s^{-1} could be rationalized by DPN. Thus, the deformation of the Ti-5V-5Mo-5Cr-4Al alloy at a very low strain rate and at moderate temperatures led to the formation of precipitates. Another important observation in Figure 2 is the effect of the deformation parameters on the ductility. The elongation at fracture increased with the increase in the deformation temperature up to a temperature of 450 °C and then decreased with a further increase in the temperature. This reduction in ductility at elevated temperatures could be rationalized by hot embrittlement being effective in the case of coarse-grained conditions at elevated temperatures [30]. Here, the grain boundaries were detrimentally affected at higher deformation temperatures, eventually leading to localized damage, fast fracture, and lower ductility.

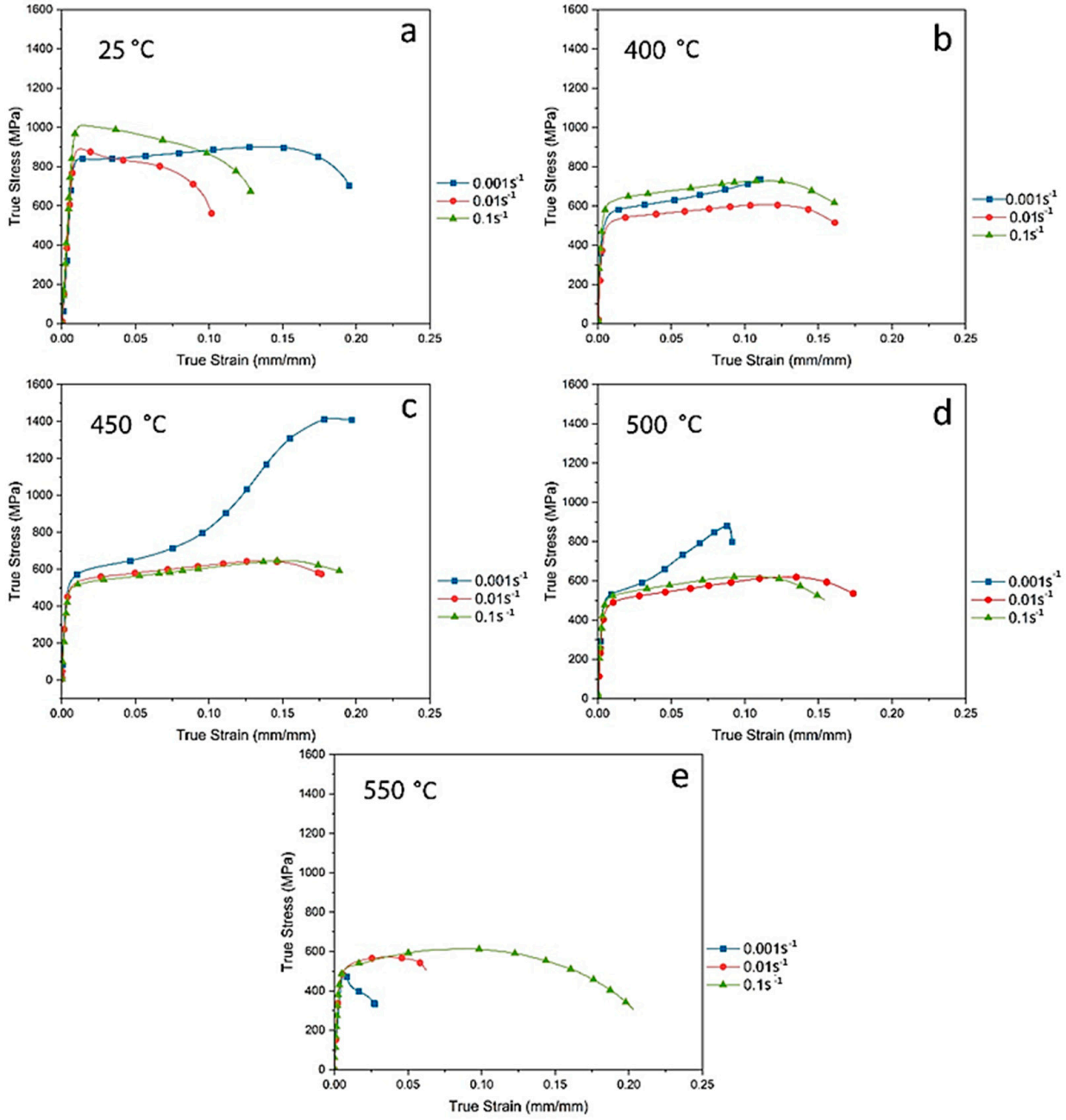

Figure 2. True stress–true strain response of Ti-5V-5Mo-5Cr-4Al alloy in tensile test applying different strain rates at (**a**) 25 °C, (**b**) 400 °C, (**c**) 450 °C, (**d**) 500 °C, and (**e**) 550 °C.

The observations made in the tensile tests were fully supported by the trends obtained from the microhardness assessment for different deformation conditions, as summarized in Table 2. The microhardness measurements of the deformed specimens were conducted close to the fractured surface, where the highest degree of plastic deformation occurred. It should be noted at this point that prior to microhardness measurements, all specimens were ground and polished to remove oxide films formed during tensile deformation at elevated temperatures. The standard deviations are also reported in Table 2. The microhardness values decreased with an increase in the deformation temperature at strain rates of 0.01 and 0.1 s^{-1}, while the microhardness of the specimens deformed at moderate temperatures with a strain rate of 0.001 s^{-1} remarkably increased. The reduction in the microhardness of the specimens deformed at higher temperatures and the increase in the microhardness of those deformed at the lowest strain rate could be attributed to the occurrence of the DRV and DPN mechanisms, respectively [7,25–29].

Table 2. Microhardness of Ti-5V-5Mo-5Cr-4Al alloy specimens in various conditions; standard deviations are provided.

Conditions	Microhardness (HV 1)
Solution treated	280 ± 2.4
400 °C and 0.1 s^{-1}	285 ± 5.1
400 °C and 0.01 s^{-1}	273 ± 6.2
400 °C and 0.001 s^{-1}	294 ± 7.9
450 °C and 0.1 s^{-1}	270 ± 5.5
450 °C and 0.01 s^{-1}	256 ± 6.9
450 °C and 0.001 s^{-1}	365 ± 7.2
500 °C and 0.1 s^{-1}	269 ± 6.4
500 °C and 0.01 s^{-1}	264 ± 1.5
500 °C and 0.001 s^{-1}	393 ± 8.1
550 °C and 0.1 s^{-1}	268 ± 3.6
550 °C and 0.01 s^{-1}	262 ± 7.5
550 °C and 0.001 s^{-1}	239 ± 8.2

3.2. Microstructure Evolution

Figure 3 shows the microstructure of the Ti-5V-5Mo-5Cr-4Al alloy specimens in different conditions. It can be seen that the solution-treated specimen consisted of equiaxed and coarse grains with an average grain size of 142 µm. It is worth noting that deforming the Ti-5V-5Mo-5Cr-4Al alloy even up to 550 °C did not result in severe grain growth. The constancy of the grain size over the course of the warm tensile tests could be imputed to the dominance of the DRV mechanism. It is well-established that grain size remains constant during the occurrence of DRV, while the DRX mechanism promotes the nucleation of recrystallized grains and possibly subsequent grain growth [26,31]. Generally, these trends in terms of grain size evolution were in line with the mechanical properties detailed above.

The microstructure of the Ti-5V-5Mo-5Cr-4Al alloy after the elevated temperature tensile test at a constant strain rate of 0.001 s^{-1} and a deformation temperature of 450 °C was analyzed by TEM (Figure 4). Dislocation substructures could be seen in the microstructure of the deformed specimen. As is well-known, DRV at moderate deformation temperatures can result in the formation of subgrains within the initial grains [32]. At a higher magnification (α), precipitates could also be seen, confirming the occurrence of DPN during elevated temperature deformation at 450 °C at a relatively low strain rate. DPN can be favored at a high level of supersaturation, while deformation occurs at moderate temperatures [33].

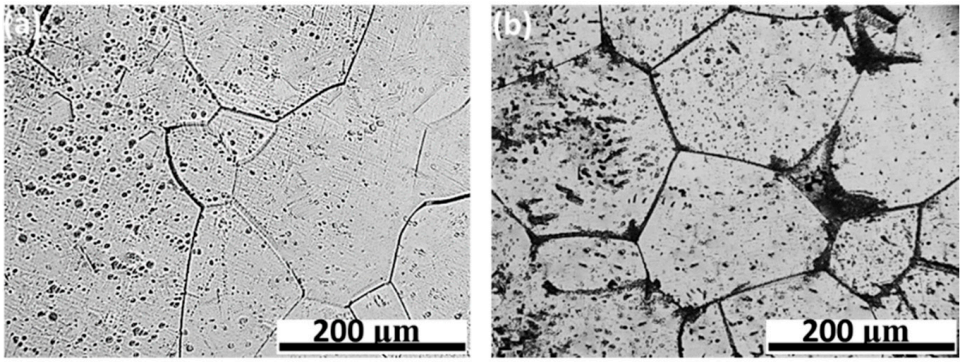

Figure 3. Microstructure of Ti-5V-5Mo-5Cr-4Al: (**a**) solution-treated and (**b**) solution-treated followed by deformation at 550 °C with a strain rate of 0.001 s^{-1}.

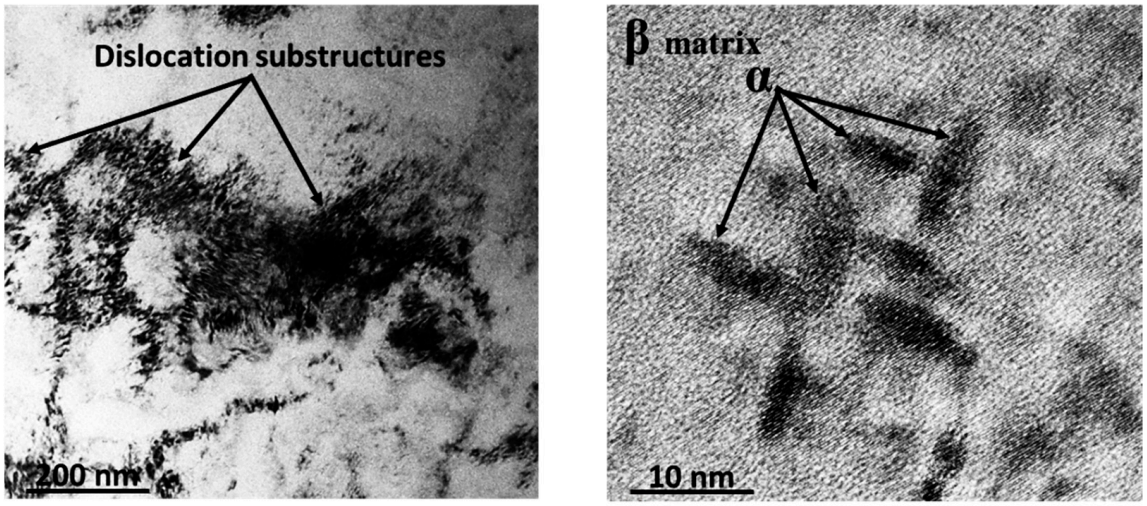

Figure 4. TEM micrographs of the specimen after the elevated temperature tensile test at a constant strain rate of 0.001 s^{-1} and a deformation temperature of 450 °C.

3.3. Fracture Surface Analysis

The effect of the deformation temperature is shown in Figure 5. The size of dimples and micro-voids increased remarkably upon an increase in temperature from 25 °C to 400 °C. At elevated temperatures, void coalescence is considered an important fracture mechanism [34]. An increase in the depth and size of dimples at higher deformation temperatures has been reported elsewhere [16,17]. Void coalescence and growth are enabled by the increase in the diffusion rate at higher deformation temperatures [35,36]. For the specimens deformed with a strain rate of 0.001 s^{-1} at 450 °C and 500 °C, a different fracture surface morphology was seen (Figure 5c,d). It is well-documented that the presence of a secondary phase in the direct vicinity of the grain boundary causes decohesion at the interface during deformation [37]. Hence, the brittle intergranular fracture observed after testing at a strain rate of 0.001 s^{-1} and moderate temperatures could be explained by localized embrittlement and decohesion, respectively. The fracture mode of the specimen deformed at 550 °C again was characterized by large dimples (Figure 5e). The observation of such a fracture mode along with the relatively poor mechanical properties of the Ti-5V-5Mo-5Cr-4Al alloy at 550 °C indicated that hot embrittlement came into play [30].

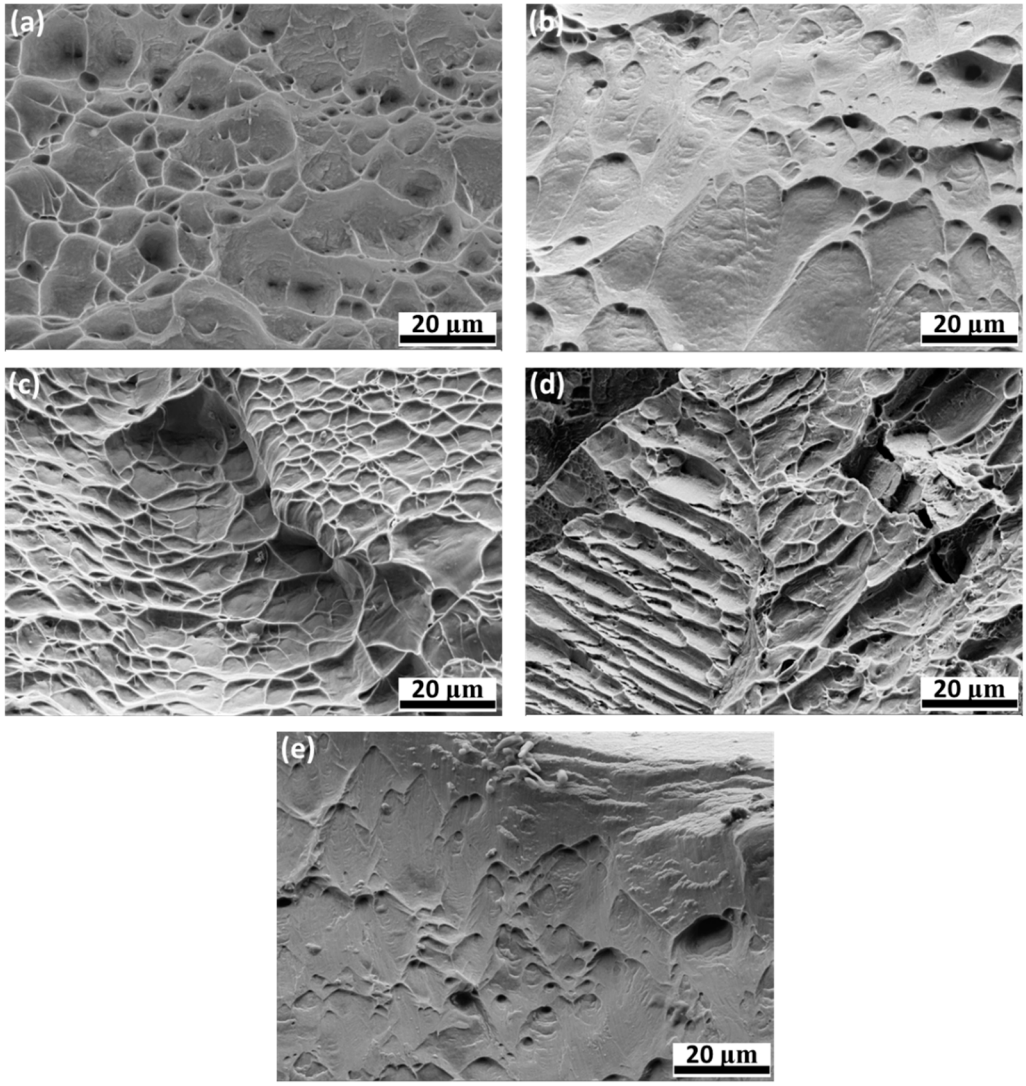

Figure 5. Fracture surface of Ti-5V-5Mo-5Cr-4Al alloy specimens: (**a**) solution-treated followed by deformation at 25 °C with a strain rate of 0.001 s^{-1}, (**b**) solution-treated followed by deformation at 400 °C with a strain rate of 0.001 s^{-1}, (**c**) solution-treated followed by deformation at 450 °C with a strain rate of 0.001 s^{-1}, (**d**) solution-treated followed by deformation at 500 °C with a strain rate of 0.001 s^{-1}, (**e**) solution-treated followed by deformation at 550 °C with a strain rate of 0.001 s^{-1}.

In order to further investigate the influence of the deformation rate on the fracture behavior of the Ti-5V-5Mo-5Cr-4Al alloy, the fracture surfaces of the specimens deformed at 400 °C and 550 °C with various strain rates are shown in Figure 6. In direct comparison, the sizes of the dimples and micro-voids were reduced with an increase in the rate of deformation. Particularly, larger voids and dimples were evident for the specimens deformed at a strain rate of 0.001 s^{-1}. The growth of dimples and voids occurred with a decrease in the strain rate since the lower rate of deformation provided sufficient time for the coalescence of micro-voids [34]. Similar to the present study, the deformation of a Ti-10-2-3 alloy at a low strain rate led to an increase in dimple size [16]. It is also worth noting that serpentine sliding was found at higher deformation temperatures (Figure 6e,f). Serpentine sliding is an indication of ductile fracture when the direction of principal stress is perpendicular to the dimples [34,38,39].

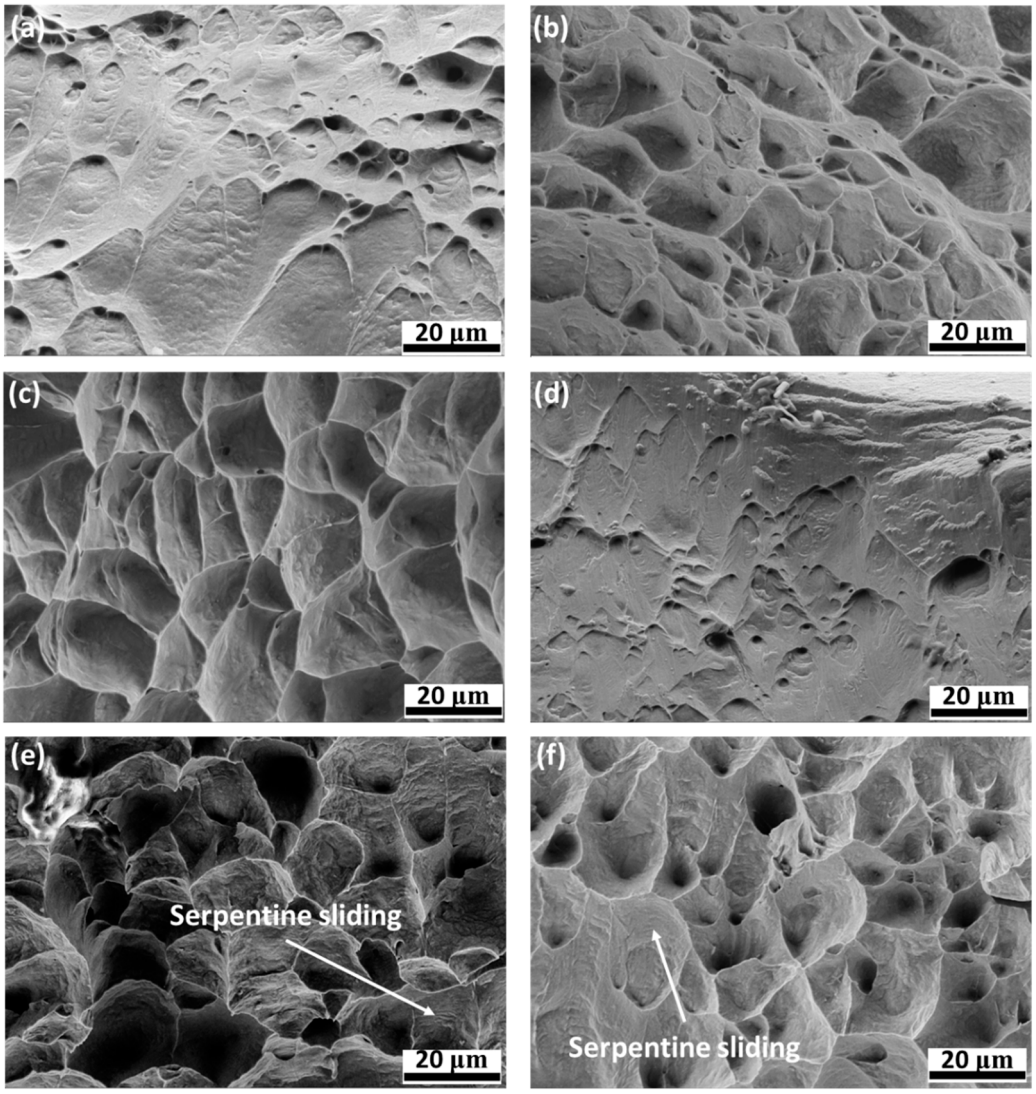

Figure 6. Fracture surface of Ti-5V-5Mo-5Cr-4Al alloy specimens: (**a**) solution-treated followed by deformation at 400 °C with a strain rate of 0.001 s^{-1}, (**b**) solution-treated followed by deformation at 400 °C with a strain rate of 0.01 s^{-1}, (**c**) solution-treated followed by deformation at 400 °C with a strain rate of 0.1 s^{-1}, (**d**) solution-treated followed by deformation at 550 °C with a strain rate of 0.001 s^{-1}, (**e**) solution-treated followed by deformation at 550 °C with a strain rate of 0.01 s^{-1}, (**f**) solution-treated followed by deformation at 550 °C with a strain rate of 0.1 s^{-1}.

3.4. Cause–Effect Relationships

The cause–effect relationships for the solution-heat-treated Ti-5V-5Mo-5Cr-4Al alloy upon warm tensile deformation are highlighted in Figure 7. As schematically shown, the deformation of the solution-heat-treated Ti-5V-5Mo-5Cr-4Al alloy at moderate temperature resulted in the occurrence of DRV. Although the temperature was not high enough for the onset of DRX, it was still high enough to reduce the stored energy by the annihilation or rearrangement of dislocations in the crystal structure [26]. As a result, a considerable reduction in the strength of the alloy occurred. Another phenomenon, so-called DPN, could have also taken place during the deformation of the solution-heat-treated Ti-5V-5Mo-5Cr-4Al alloy at moderate temperatures. Based on the experiments conducted in the present study, DPN could occur during the warm deformation of the alloy in the case of low strain rates. As the specimens were deformed in the $\alpha + \beta$ phase zone, the formation of α precipitates was expected [40]. The formation of the α phase during DPN is thought to result in the strengthening of the alloy, since α precipitates can impede dislocation

movements [41]. The results obtained in the present study clearly indicated that the warm deformation characteristics of the solution-heat-treated Ti-5V-5Mo-5Cr-4Al alloy were governed by a combination of DRV and DPN phenomena.

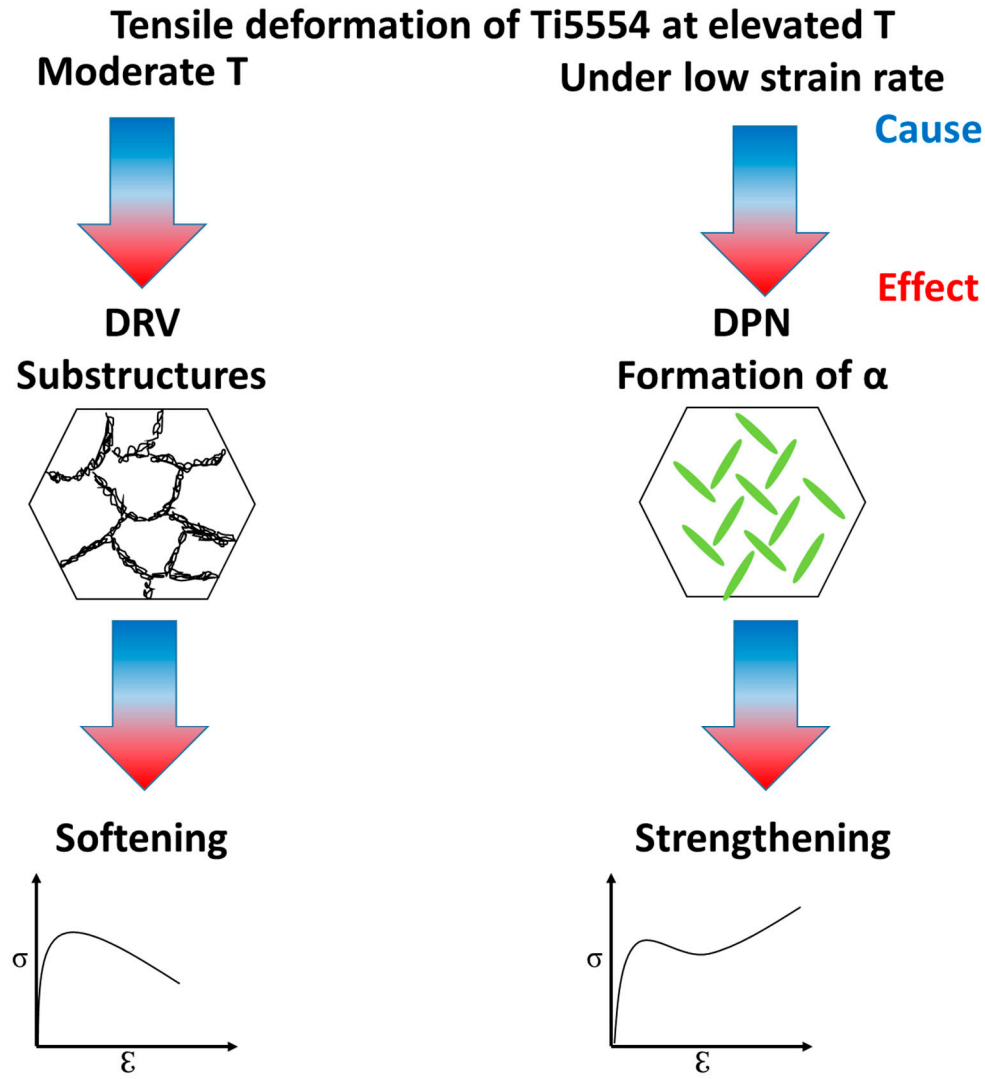

Figure 7. Schematic detailing cause–effect relationships for the solution-heat-treated Ti-5V-5Mo-5Cr-4Al alloy upon warm tensile deformation.

4. Conclusions

The mechanical and fracture characteristics of a Ti-5V-5Mo-5Cr-4Al alloy were studied in various deformation conditions in a cold-to-warm working regime. From the results presented above, the following conclusions could be drawn:

(i). The flow stress was sensitive to the deformation temperature and rate. At strain rates of 0.1 s^{-1} and 0.01 s^{-1}, the true UTS levels decreased with an increase in temperature. At the lowest rate of deformation, the flow stress level showed a considerable increase at intermediate temperatures.

(ii). Microhardness data, optical microscopy investigations, and TEM studies confirmed that the DRV mechanism was responsible for the softening of the alloy in the temperature range considered.

(iii). The TEM analysis of the deformed specimens revealed that dynamic precipitation occurred at a strain rate of 0.001 s^{-1}, leading to the enhancement of the peak strength levels. Elevated temperature deformation was accompanied by void growth and

coalescence, and these effects were mostly pronounced at higher temperatures and lower strain rates.

(iv). It was demonstrated that by selecting various deformation parameters, the deformation behavior could be governed by DRV (at moderate temperatures) or DPN (at moderate temperatures and low rates of deformation).

Author Contributions: S.V.S.: conceptualization; methodology; data curation; investigation; writing (original draft, review, and editing). H.J.M.: resources; project administration; writing (review and editing); supervision. T.N.: resources; project administration; writing (review and editing); supervision. G.G.Y.: conceptualization; methodology; investigation; resources; funding acquisition; project administration; writing (review and editing); supervision. All authors have read and agreed to the published version of the manuscript.

Funding: This research received no external funding.

Institutional Review Board Statement: Not applicable.

Informed Consent Statement: Not applicable.

Data Availability Statement: The data that support the findings of this study are available upon request.

Acknowledgments: The support of Roketsan Inc. is gratefully acknowledged.

Conflicts of Interest: The authors declare no conflict of interest.

References

1. Duerig, T.W.; Terlinde, G.T.; Williams, J.C. Phase transformations and tensile properties of Ti-10V-2Fe-3AI. *Metall. Trans. A* **1980**, *11*, 1987–1998. [CrossRef]
2. Hua, K.; Xue, X.; Kou, H.; Fan, J.; Tang, B.; Li, J. Characterization of hot deformation microstructure of a near beta titanium alloy Ti-5553. *J. Alloys Compd.* **2014**, *615*, 531–537. [CrossRef]
3. Lee, W.-S.; Lin, C.-F. Plastic deformation and fracture behaviour of Ti–6Al–4V alloy loaded with high strain rate under various temperatures. *Mater. Sci. Eng. A* **1998**, *241*, 48–59. [CrossRef]
4. Jones, N.G.; Dashwood, R.J.; Dye, D.; Jackson, M. The Flow Behavior and Microstructural Evolution of Ti-5Al-5Mo-5V-3Cr during Subtransus Isothermal Forging. *Metall. Mater. Trans. A* **2009**, *40*, 1944–1954. [CrossRef]
5. Sajadifar, S.V.; Yapici, G.G. Hot Deformation Behavior of Ultra-Fine Grained Pure Ti. *Adv. Mater. Res.* **2013**, *829*, 10–14. [CrossRef]
6. Sajadifar, S.V.; Yapici, G.G. Effect of Purity Levels on the High-Temperature Deformation Characteristics of Severely Deformed Titanium. *Metall. Mater. Trans. A* **2017**, *48*, 999–1012. [CrossRef]
7. Sajadifar, S.V.; Yapici, G.G. Workability characteristics and mechanical behavior modeling of severely deformed pure titanium at high temperatures. *Mater. Des.* **2014**, *53*, 749–757. [CrossRef]
8. Sajadifar, S.V.; Yapici, G.G. Elevated temperature mechanical behavior of severely deformed titanium. *J. Mater. Eng. Perform.* **2014**, *23*, 1834–1844. [CrossRef]
9. Sajadifar, S.V.; Atli, C.; Yapici, G.G. Effect of severe plastic deformation on the damping behavior of titanium. *Mater. Lett.* **2019**, *244*, 100–103. [CrossRef]
10. Sajadifar, S.V.; Yapici, G.G.; Demler, E.; Krooß, P.; Wegener, T.; Maier, H.J.; Niendorf, T. Cyclic deformation response of ultra-fine grained titanium at elevated temperatures. *Int. J. Fatigue* **2019**, *122*, 228–239. [CrossRef]
11. Sajadifar, S.V.; Wegener, T.; Yapici, G.G.; Niendorf, T. Effect of grain size on the very high cycle fatigue behavior and notch sensitivity of titanium. *Theor. Appl. Fract. Mech.* **2019**, *104*, 102362. [CrossRef]
12. Sajadifar, S.V.; Maier, H.J.; Niendorf, T.; Yapici, G.G. Fracture Behavior of Ultrafine-Grained Titanium Under Tension at Elevated Temperatures. *J. Eng. Mater. Technol.* **2020**, *142*, 4047747. [CrossRef]
13. Sajadifar, S.V.; Yapici, G.G. High Temperature Flow Response Modeling of Ultra-Fine Grained Titanium. *Metals* **2015**, *5*, 1315–1327. [CrossRef]
14. Lee, W.-S.; Kao, C.-H. Hot deformation behaviour and microstructural evolution of biomedical Ti-13Nb-13Zr alloy in high strain rate range. *Mater. Sci. Eng. A* **2016**, *677*, 230–239. [CrossRef]
15. Zhan, H.; Wang, G.; Kent, D.; Dargusch, M. The dynamic response of a metastable β Ti–Nb alloy to high strain rates at room and elevated temperatures. *Acta Mater.* **2016**, *105*, 104–113. [CrossRef]
16. Bobbili, R.; Madhu, V. Effect of strain rate and stress triaxiality on tensile behavior of Titanium alloy Ti-10-2-3 at elevated temperatures. *Mater. Sci. Eng. A* **2016**, *667*, 33–41. [CrossRef]
17. Zhao, H.; Lu, B.; Tong, M.; Yang, R. Tensile behavior of Ti-22Al-24Nb-0.5Mo in the range 25–650 °C. *Mater. Sci. Eng. A* **2017**, *679*, 455–464. [CrossRef]
18. Seifi, M.; Salem, A.; Satko, D.; Shaffer, J.; Lewandowski, J.J. Defect distribution and microstructure heterogeneity effects on fracture resistance and fatigue behavior of EBM Ti–6Al–4V. *Int. J. Fatigue* **2017**, *94*, 263–287. [CrossRef]

19. Huang, C.; Zhao, Y.; Xin, S.; Tan, C.; Zhou, W.; Li, Q.; Zeng, W. High cycle fatigue behavior of Ti–5Al–5Mo–5V–3Cr–1Zr titanium alloy with lamellar microstructure. *Mater. Sci. Eng. A* **2017**, *682*, 107–116. [CrossRef]
20. Chen, Y.; Zhang, K.; Hu, X.; Lei, Z.; Ni, L. Study on laser welding of a Ti-22Al-25Nb alloy: Microstructural evolution and high temperature brittle behavior. *J. Alloys Compd.* **2016**, *681*, 175–185. [CrossRef]
21. Wu, G.Q.; Shi, C.L.; Sha, W.; Sha, A.X.; Jiang, H.R. Microstructure and high cycle fatigue fracture surface of a Ti–5Al–5Mo–5V–1Cr–1Fe titanium alloy. *Mater. Sci. Eng. A* **2013**, *575*, 111–118. [CrossRef]
22. Schmidt, P.; El-Chaikh, A.; Christ, H.-J. Effect of Duplex Aging on the Initiation and Propagation of Fatigue Cracks in the Solute-rich Metastable β Titanium Alloy Ti 38-644. *Metall. Mater. Trans. A* **2011**, *42*, 2652–2667. [CrossRef]
23. Quan, G.-Z.; Zou, Z.-Y.; Wu, D.-S.; Liang, J.-T. Prediction of ductile fracture initiation for Ti–10V–2Fe–3Al alloy by compressions at different temperatures and strain rates. *Mater. High Temp.* **2016**, *33*, 6–14. [CrossRef]
24. *ASTM E8/E8M*; 16a Standard Test Methods for Tension Testing of Metallic Materials. ANSI: Washington, DC, USA, 2016.
25. Bhargava, A.K.; Sharma, C.P. *Mechanical Behaviour and Testing of Materials*; PHI Learning Private Ltd.: Delhi, India, 2011; ISBN 9788120342507.
26. McQueen, H.J. Dynamic Recovery and Recrystallization. In *Encyclopedia of Materials: Science and Technology*; Elsevier: Amsterdam, The Netherlands, 2001; pp. 2375–2381. ISBN 9780080431529.
27. Lin, Y.C.; Xia, Y.C.; Jiang, Y.Q.; Zhou, H.M.; Li, L.T. Precipitation hardening of 2024-T3 aluminum alloy during creep aging. *Mater. Sci. Eng. A* **2013**, *565*, 420–429. [CrossRef]
28. Lin, Y.C.; Jiang, Y.Q.; Chen, X.M.; Wen, D.X.; Zhou, H.M. Effect of creep-aging on precipitates of 7075 aluminum alloy. *Mater. Sci. Eng. A* **2013**, *588*, 347–356. [CrossRef]
29. Song, Z.Y.; Sun, Q.Y.; Xiao, L.; Sun, J.; Zhang, L.C. Precipitation behavior and tensile property of the stress-aged Ti-10Mo-8V-1Fe-3.5Al alloy. *Mater. Sci. Eng. A* **2011**, *528*, 4111–4114. [CrossRef]
30. Li, J.; Jiang, B.; Zhang, C.; Zhou, L.; Liu, Y. Hot embrittlement and effect of grain size on hot ductility of martensitic heat-resistant steels. *Mater. Sci. Eng. A* **2016**, *677*, 274–280. [CrossRef]
31. Souza, R.C.; Silva, E.S.; Jorge, A.M.; Cabrera, J.M.; Balancin, O. Dynamic recovery and dynamic recrystallization competition on a Nb- and N-bearing austenitic stainless steel biomaterial: Influence of strain rate and temperature. *Mater. Sci. Eng. A* **2013**, *582*, 96–107. [CrossRef]
32. Furuhara, T.; Toji, Y.; Abe, H.; Maki, T. Dynamic Recovery and Recrystallization in Beta-Titanium Alloys. *Mater. Sci. Forum* **2003**, *426–432*, 655–660. [CrossRef]
33. Sajadifar, S.V.; Scharifi, E.; Weidig, U.; Steinhoff, K.; Niendorf, T. Performance of Thermo-Mechanically Processed AA7075 Alloy at Elevated Temperatures—From Microstructure to Mechanical Properties. *Metals* **2020**, *10*, 884. [CrossRef]
34. Zhou, M.; Lin, Y.C.; Deng, J.; Jiang, Y.-Q. Hot tensile deformation behaviors and constitutive model of an Al–Zn–Mg–Cu alloy. *Mater. Des.* **2014**, *59*, 141–150. [CrossRef]
35. Sabirov, I.; Valiev, R.Z.; Semenova, I.P.; Pippan, R. Effect of Equal Channel Angular Pressing on the Fracture Behavior of Commercially Pure Titanium. *Metall. Mater. Trans. A* **2010**, *41*, 727–733. [CrossRef]
36. Smallman, R.E.; Bishop, R.J.; Ray, J. *Metals and Materials: Science, Processes, Applications*; Butterworth-Heinemann: Oxford, UK, 1995; ISBN 075061093X.
37. Fukuda, T. Effect of Titanium Carbide Precipitates on the Ductility of 30 mass% Chromium Ferritic Steels. *Mater. Trans.* **2003**, *44*, 1153–1158. [CrossRef]
38. Xiao, Z.; Huang, Y.; Liu, H.; Wang, S. Hot Tensile and Fracture Behavior of 35CrMo Steel at Elevated Temperature and Strain Rate. *Metals* **2016**, *6*, 210. [CrossRef]
39. Deng, J.; Lin, Y.C.; Li, S.-S.; Chen, J.; Ding, Y. Hot tensile deformation and fracture behaviors of AZ31 magnesium alloy. *Mater. Des.* **2013**, *49*, 209–219. [CrossRef]
40. Fu, Q.; Yuan, W.; Xiang, W. Dynamic Softening Mechanisms and Microstructure Evolution of TB18 Titanium Alloy during Uniaxial Hot Deformation. *Metals* **2021**, *11*, 789. [CrossRef]
41. Kar, S.K.; Suman, S.; Shivaprasad, S.; Chaudhuri, A.; Bhattacharjee, A. Processing-microstructure-yield strength correlation in a near β Ti alloy, Ti–5Al–5Mo–5V–3Cr. *Mater. Sci. Eng. A* **2014**, *610*, 171–180. [CrossRef]